Parameter identification problem in bimaterial human skin and sensitivity analysis : Uncertainties in biomechanics of skin.

D. SUTULA[a], A. ELOUNEG[a], M. SENSALE[a,b], F. CHOULY[c], J. CHAMBERT[a], A. LEJEUNE[a], D. BAROLI[b], P. HAUSEUX[b], S. BORDAS[b], E. JACQUET[a,⋆]

a. Univ. Bourgogne Franche-Comté, FEMTO-ST Institute, Department of Applied Mechanics, Besançon, France.
b. University of Luxembourg, Institute of Computational Engineering, Luxembourg.
c. Univ. Bourgogne Franche-Comté, Institut de Mathématiques de Bourgogne, Dijon, France.
⋆ Corresponding author, emmanuelle.jacquet@univ-fcomte.fr

Résumé :

Le travail proposé concerne la prédiction de la réponse numérique d'une structure biomécanique soumise à un état de chargement externe inconnu. La méthodologie s'appuie sur la modélisation de structures homogènes puis hétérogènes, telles que des tissus cutanés sains ou pathologiques accessibles expérimentalement et soumis à des conditions aux limites partiellement connues. Les données expérimentales correspondent à une extension d'une zone de peau située entre deux patins dont le déplacement relatif est imposé. Ces données constituent les données d'entrée du modèle numérique. Ce sont la force de réaction sur un patin et le champ de déplacement de la surface de la peau située entre les deux patins et tout autour. Le modèle numérique consiste en une représentation de la géométrie du domaine bi-matériau pour lequel les lois de comportement de type neo-hookéen sont utilisées. Les conditions aux limites et de chargement sont celles du test expérimental. Les paramètres des lois de comportement des 2 matériaux sont identifiés par méthode inverse à partir d'une fonction d'objectif minimizant l'écart entre les champs des déplacements calculés et ceux mesurés par corrélation d'images sous la contrainte de réduire l'écart entre la force de réaction calculée et celle mesurée sur le patin. Une analyse de la sensibilité du modèle aux paramètres matériau est présentée.

Abstract :

The proposed paper concerns the prediction of the numerical response of a biomechanical structure submitted to an unknown external loading state. The methodology is based on homogeneous and then heterogeneous structures such as healthy or pathological cutaneous tissues that can be mechanically tested in vivo under a patchy knowledge of boundary conditions. Experimental data corresponding to the extension of a piece of skin located between two pads with displacement enslavement, represent input data to the numerical model. Data are reaction force on one pad and displacement field between *the two pads and all around. The numerical model consists of a representation of the bi-material domain geometry with neo-hookean behaviors. The boundary conditions and loadings of the experimental extension test are imposed. The materials parameters have been identified by inverse method starting from a constrained cost function minimizing the difference between the calculated displacements field and experimental displacements field obtained by digital image correlation and taking into account the reaction force as a constraint. An analysis of the model sensitivity to material parameters is presented.*

Key words : Mechanical behaviour ; Human skin, Inverse method

1 Introduction

Biomechanics nowdays largely covers many fields of mechanics and combines the various complexities related to.

Our focus is on the patient-specific biomechanical characterisation of human skin with a keloid scar (Fig. 1).

FIGURE 1 – Keloid scar located on the left-upper arm ($X = 15$ mm, $Y = 47$ mm).

Keloids are non-cancerous tumours [1] that grow continuously on the skin. The evolution of keloids is known to be related to genetic, biological, biophysical, and biomechanical factors [2]. In our work, we focus on the latter type of influence ; for example, the state of stress inside a keloid and in the surrounding skin is known to play a significant role in the growth of the keloid [2].

2 Materials and Methods

2.1 Material problem

To characterize the mechanical behaviour of a bi-material structure composed of healthy skin and keloid skin, a suitable material model has been chosen. *In vivo* experiments are carried out using a custom-made extensometer [3] to obtain N_E data points : $k = 1, 2, \dots, N_E$, of the applied force $\bar{f}^k$ and the resulting surface displacement field $\bar{u}^k$. The surface displacements are determined using a digital image correlation (DIC) technique (Fig. 2). As shown in figure (3), the DIC measurement domain limits are far beyond the limited zone where the inverse identification is performed. This would help to reduce noises.

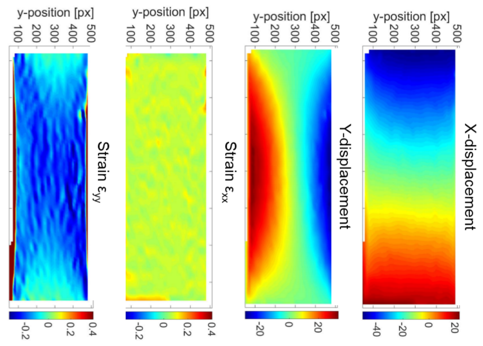

FIGURE 2 – Reference displacement fields obtained by digital image correlation and the post-processed strain fields. Fields for healthy skin

The numerical model consists of a finite element discretisation of the part of the skin with the keloid. A keloid is observed on a patient using ultrasound imaging and optical microscopy. The 3D image of the surface is used to develop the keloid-skin geometrical model (Fig. 3). The model domain Ω is divided into two sub-domains $\Omega_1 \cup \Omega_2 = \Omega$.

2.2 Optimization problem

For the chosen hyperelastic material model(s) with a total of N_m model parameters we look for the parameters m that minimise the mismatch between the experimental $u^{(k)}_{\text{msr}}$ and the numerical $u^{(k)}$ observations of the displacements on the surface of the skin Γ_E subject to quasi-static equilibrium $F(u^{(k)}, m; v) = 0 \quad \forall v \in V$ on all loading steps $k = 1, 2, \ldots, N_E$. V is the space of admissible virtual displacements.

In vivo extensometer experiments are controlled with prescribed displacement of the pad [3]. In this case, the measured force $f^{(k)}_{\text{msr}}$ needs to be introduced into the cost functional in a form of a constraint equation. This can be done using the Lagrange multiplier method. By introducing a single multiplier λ the reaction force constraint can be enforced on average over all times. The problem is then to find the stationary points of $J(m, \lambda) = \sum_{k=1}^{N_E} J^{(k)}(m, \lambda)$. The optimization problem is defined as :

$$\hat{m} = \underset{m,\lambda \in \mathbb{R}^{N_m+1}}{\operatorname{argmin}} \sum_{k=1}^{N_E} J^{(k)}(m, \lambda) \tag{1}$$

$$\text{subject to : } F(u^{(k)}, m; v) = 0 \quad \forall v \in V \tag{2}$$

where

$$J^{(k)}(m, \lambda) = J(u^{(k)}(m), m, \lambda) := \int_{\Gamma^u_{\text{msr}}} \left(u^{(k)}(m) - u^{(k)}_{\text{msr}} \right)^2 dx + \lambda \int_{\Gamma^f_{\text{msr}}} \left(f(u^{(k)}(m), m) - f^{(k)}_{\text{msr}} \right) dx \tag{3}$$

with Γ^u_{msr} a part of the domain Γ_E where the displacement field is measured (i.e. using Digital Image Correlation) and Γ^f_{msr} the boundary where the force is measured using deformation gauge. the problem defined by equations (1) and (2) can be solved using Newton's method.

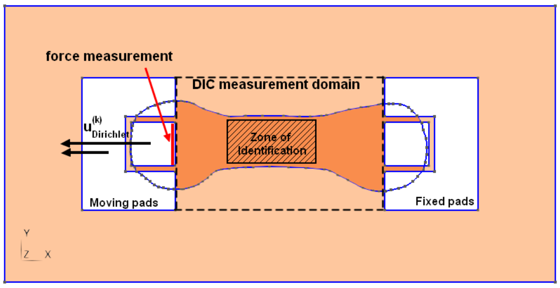

FIGURE 3 – Geometry model and boundaries conditions of keloid/skin characterisation

For the sake of brevity suppose the material model parameters and any constraint multipliers can be collectively denoted by $\bar{m}_i$ for $i = 1, 2, ..., N_{\bar{m}}$ where in the case of a single constraint multiplier $N_{\bar{m}} = N_m + 1$. In this case the gradient of the cost at load-step $k = 1, 2, \ldots, N_E$ can be expressed as :

$$D_{\bar{m}_i} J^{(k)} = \partial_u J(u^{(k)}, \bar{m})[D_{\bar{m}_i} u^{(k)}] + \partial_{\bar{m}_i} J(u^{(k)}, \bar{m}) = 0 \quad \forall i = 1, 2, \ldots, N_{\bar{m}} \tag{4}$$

Similarly, the Hessian of the model cost can be expressed as :

$$\begin{aligned} D^2_{\bar{m}_i\,\bar{m}_j} J^{(k)} = {} & \partial_u J[D^2_{\bar{m}_i\,\bar{m}_j} u^{(k)}] + \partial^2_{uu} J[D_{\bar{m}_i} u^{(k)}, D_{\bar{m}_j} u^{(k)}] \\ & + \partial_{\bar{m}_i u} J[D_{\bar{m}_j} u^{(k)}] + \partial^2_{u\bar{m}_j} J[D_{\bar{m}_i} u^{(k)}] + \partial^2_{\bar{m}_i\bar{m}_j} J \end{aligned} \tag{5}$$

Usually, the derivatives $D_{\bar{m}_i} u$ and $D^2_{\bar{m}_i\,\bar{m}_j} u$ are not computed explicitly ; instead, the adjoint solution method is involved thereby enabling one to compute $D_{\bar{m}_i} J^{(k)}$ and $D^2_{\bar{m}_i\,\bar{m}_j} J^{(k)}$ directly and efficiently.

It is also possible to perform the optimization at each time and determine the locally optimal model parameters. This can be of interest since the local model parameter deviations from the globally optimal values can serve as a good indication of the fitness of a particular hyperelastic model to approximate the biological tissue at hand.

2.3 Model parameters sensitivities

Goal of this study is to determine model parameters $\hat{m}$ minimizing the cost functional $J(m)$ depending on measurements obtained from a DIC analysis. As the precision of the measurements can not be trusted in general, we seek to study the sensitivity of the inferred model parameters to measurement noise. To this end, an artificial noise function can be superposed on the true measurements and the sensitivity of the model parameters to the noise function can be analyzed using automatic differentiation tools within the computational framework. The model parameter sensitivities δm with respect to a noise function $v_{msr}^{(k)}$ at pseudo-time k can be computed as :

$$\left\{ \frac{\partial m}{\partial v_{msr}^{(k)}} \right\} = - \left[\frac{d^2 J}{dm^2} \right]^{-1} \left\{ \frac{d^2 J^{(k)}}{\partial v_{msr}^{(k)} dm} \right\} \tag{6}$$

The noise function can be one for the measured displacement field or one for the measured reaction force. In the case of the displacement field uncertainty, the model parameter sensitivities can be projected on a scalar function space to yield plots indicating where a particular model parameter is most sensitive to the measured displacements. For example, Fig. 4 shows the sensitivity of the generalized Poisson's parameter in the Neo-Hookean hyper-elastic material model.

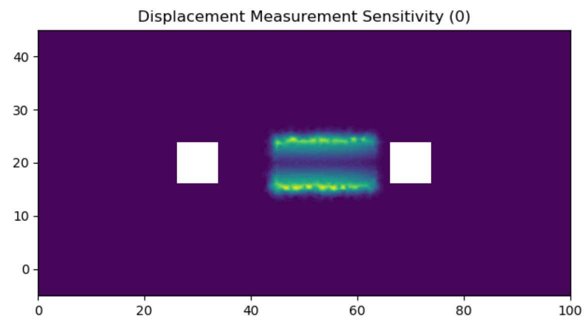

FIGURE 4 – Poisson's parameter sensitivity due to the measured displacement field at the final time-step.

Subsequently, the suitability of a chosen material model can been assessed by quantifying the sensitivity of the model parameters with respect to the noise in the measurement data. Consequently, equation 6 can be used to assess the fitness of a particular material model for the skin-keloid tissue considering the noise in the experimental measurement data.

3 Application

Figure 5 describes the numerical process from experimental data to outputs like model parameters for skin and surroundig healthy skin and true stress fields. This overall process has been implemented using python packages for data preprocessing (filtering, projection on mesh) and FEniCs tool for the Finite Element simulation. Identification and sensitivity analysis has been implemented in python.

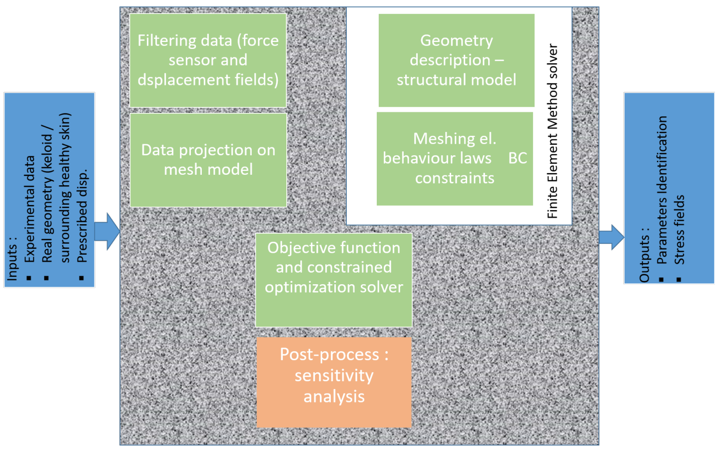

FIGURE 5 – Numerical process

For the estimation of the model parameters, an inverse solution strategy to best fit the model to a set of experimental measurements of the skin-keloid mechanical response due to different loading conditions has been applied. Finite element model of extensometer experiment is illustrated in Figure 6. Extension is controlled by the two pads (grey squares). They are modelised like rigid holes. One is uniaxially translated in the longitudinal direction ($u_x = u_x^{prescribed}$), the second is fixed ($u_x = 0$). External boundaries are such that top and bottom are fixed and right and left are constrained to $u_y = 0$. All the blue domain is meshed but only the rectangular area with apparent elements is used for identification process.

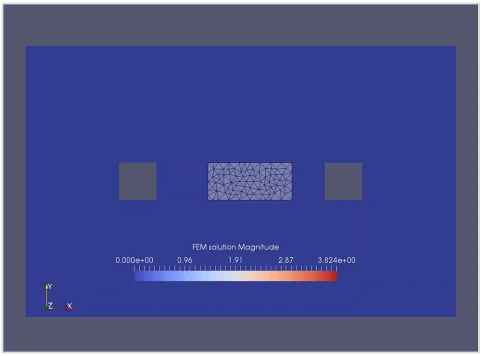

FIGURE 6 – Model with external boundaries : fixed top and bottom and $u_y = 0$

Subsequently, the suitability of a chosen material model has been assessed by quantifying the sensitivity of the model parameters with respect to the noise in the measurement data (Fig. 7).

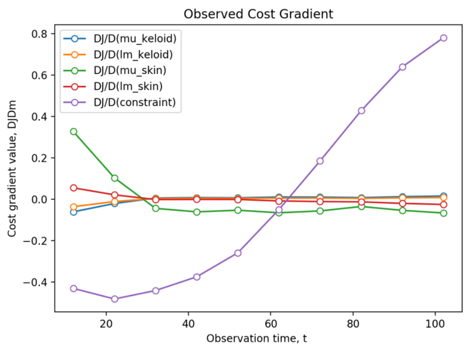

FIGURE 7 – Objective functional derivative values, DJ/Dm, at different observation times, t

After parameters identification from minimization of the cost function, a comparison between raw data reaction force and numerical reaction force calculated has exhibited a satisfactory correlation for the beginning of the extension (deformation of 8% or less) and a lack of correlation for higher deformations.

4 Discussion and Conclusion

Inverse least square method has been implemented for the uniaxial extension test of a bi-material structure and with simple hyperelastic model. More complex material models able to take into account incompressibility constraint, like Higher order Mooney-Rivlin model should bring more accurate results. The procedure consists in computing sensitivities of model parameters with respect to measurement noise of different models. Furthermore, the sensitivity analysis can be useful in the design of the experiments in order to maximize the information gained from the measurements. Note that there are some problems with high level of noise into experimental data. That's why it seems to be necessary to filter data before inverse analysis. After improvements done to the numerical model, the results can be used for predicting stress fields around the keloid scar and bring the mechanical basis of predicting the preferential directions of its growth. The ultimate goal consists in defining the specifications of a predictive device. Hereafter this concrete example, the focus of the paper has been on the analysis processing able to solve a large variety of problems from raw experimental data to robust mechanical simulations in which measurements that can be obtained are highly variable and several boundary conditions are totally unknown.

Références

[1] R. Ogawa, D.P. Orgill, Mechanobiology of cutaneous wound healing and scarring, in : Bioengineering Research of Chronic Wounds, Springer, Berlin, Heidelberg, 2009, pp. 31–42.

[2] J. Chambert, L. Zhao, D. Remache, E. Jacquet, Numerical analysis of keloid scar in the presternal area. Computer Methods in Biomechanics and Biomedical Engineering, 15 (2012) 23–24.

[3] E. Jacquet, S. Joly, J. Chambert, K. Rekik, P. Sandoz, Ultra-light extensometer for the assessment of the mechanical properties of the human skin in vivo, Skin Research and Technology, 23 (2017) 531–538.